Theoretical and Applied Climatology (2022) 149:1431–1450
https://doi.org/10.1007/s00704-022-04122-4

ORIGINAL PAPER

Southeastern Brazil inland tropicalization: Köppen system applied for detecting climate change throughout 100 years of meteorological observed data

Clayton Alcarde Alvares[1] · Paulo Cesar Sentelhas[2] · Henrique Boriolo Dias[2,3]

Received: 16 August 2021 / Accepted: 10 June 2022 / Published online: 22 June 2022

Abstract

Many regions around the world are facing climate changes, with substantial increase in air temperature over the past decades, which is mainly related to continental and global warming forced by the higher greenhouse gas (GHG) emissions. The objectives of this study were to use the Köppen climate classification to detect local climate change based on a historical series of 100 years and to assess if such change is related to those that are occurring in other spatial scales as a likely consequence of increasing GHG. This paper brings a content full of innovative results. The study area presented an average annual air temperature increase by 0.9 °C between 1917 and 2016, rising from 21.4 °C for the first climatological normal (1917–1946) to 22.3 °C for the last one (1987–2016). Furthermore, in the summer months, the temperature rose from 24.5 to 25.3 °C, and in the winter months, such increase was from 17.1 (1917–1946) to 18.3 °C (1987–2016). Our findings showed the subtropical conditions (Cfa in Köppen's classification) in the study area persisted from the beginning of the analysis (1917–1946) until the climatological normal of 1979–2008, with a clear tendency of tropicalization after that with a change in the climate type of Piracicaba from subtropical to tropical, which can now be classified as tropical with dry winter (Aw climate type). The local average air temperature showed concordances with the long-term air temperature anomalies from regional, continental, and global scales, indicating that all of them may be linked with increasing GHG emissions, since well-defined long-term linear relationships ($r^2 = 0.99$) were observed between continental and global average air temperature anomalies and atmospheric CO_2 concentration observed at the NOAA Lab in Mauna Loa in the last 59 years. While the local and regional forcing effects remain to be fully unraveled, our study provided a valid and strong scientific sound evidence that climate change occurred in Piracicaba, southeastern Brazil, in the last 100 years.

1 Introduction

Centennial weather stations are considered by scientists as an open-air museum. These stations have played a key role in the development and utilization of climate resources for farming planning, civil construction, urban and rural risk assessment, ecology, public health, tourism, and studying the climate variability and change by climatologists. A ground weather station is a facility of a very well-defined layout equipped with instruments for gauging atmospheric conditions to provide data for studies about past, present, and future climate conditions and for weather and climate forecasts (Pereira et al. 2002). The maintenance of an operational weather station for collection and recording of data during many consecutive decades are undoubtedly a challenge that can only be achieved through a lot of institutional commitment. Long-term meteorological data series can be considered as a technical and scientific patrimony

In memory of Paulo Cesar Sentelhas.

✉ Clayton Alcarde Alvares
caalvares@yahoo.com.br

Paulo Cesar Sentelhas
pcsentel.esalq@usp.br

Henrique Boriolo Dias
henrique.bdias@yahoo.com.br

[1] College of Agricultural Sciences (FCA), São Paulo State University (UNESP), Av. Universitária, 3780. 18610-034, Botucatu, SP, Brazil

[2] Luiz de Queiroz" College of Agriculture (ESALQ), University of São Paulo (USP), Av. Pádua Dias, 235. 13418-900, Piracicaba, SP, Brazil

[3] Interdisciplinary Center of Energy Planning (NIPE), University of Campinas (UNICAMP), R. Cora Coralina, 330. 13083-896, Campinas, SP, Brazil

of an institution and location since they represent the history of atmospheric conditions through the years. The well-preserved old conventional weather stations that still are in operation in their original sites are absolutely an irreplaceable climate legacy (Xue et al. 2021).

In Brazil, there were many hundreds of ground weather stations settled at the beginning of the twentieth century primarily across in the state of São Paulo (DAEE—Department of Water and Electric Energy of State of São Paulo, www.daee.sp.gov.br) and in the Northeast region of the country (DNOCS—Brazilian National Department of Works Against the Droughts, https://antigo.dnocs.gov.br). Those weather stations today would have more than 100 years of continuous observed data if their operations had not been discontinued. Hence, in the tide of meteorological observation automation, only a couple dozens of valuable centennial weather stations remain in operation in few climatic regions (https://bdmep.inmet.gov.br). These weather stations have been essential to build the national climatological database and to support the climatological normals of 1901–1930, 1931–1960, 1961–1990, 1981–2010, and 1991–2020 (Brasil 1970, 1992; Ramos et al. 2009; Diniz et al. 2018), for the construction and maintenance of the World Meteorological Organization (WMO, www.wmo.int) centennial weather stations, supporting important studies in South America (Alvares et al. 2013; Saurral et al. 2017; Díaz et al. 2021), and providing dataset for the worldwide climatological databases (Jones et al. 2012; Becker et al. 2013; Harris et al. 2014; Fick and Hijmans 2017; Castellanos-Acuna and Hamann 2020).

Based on long-term meteorological observations, ecological experiments, and modelling frameworks, climatologists have high confidence that global temperatures have increased in the past years and will continue to rise for decades to come (Chou et al. 2014; Dubreuil et al., 2018; Venegas-González et al. 2018; Bitencourt et al. 2020; Regoto et al. 2021). They are concerned about the effects that climate variability and change may have on several human activities and, also, on the Earth system. To better understand such effects, it is important to provide an overview of the basic concepts of climate variability and change because they impact the above-mentioned activities in distinct ways. Climate variability refers to the oscillations of weather conditions that are observed within the year and between the years, which are called intra-annual and inter-annual climate variability, respectively. The weather conditions, represented by air temperature, relative air humidity, incoming solar radiation, wind speed, and rainfall, are very dynamic and thus change all the time (hourly, daily, weekly, monthly up to yearly) (Alvares et al. 2021). Weather conditions are influenced by several factors, particularly by those related to the location (latitude, longitude, altitude, continentality), and the atmospheric circulation systems that are in South America are cold fronts, tropical storms, intertropical convergence zone (ITCZ), and South Atlantic convergence zone (SACZ), among others (Cavalcanti and Kousky 2009; Dias and Silva 2009). On the other hand, climate is considered as a long-term average of weather conditions, comprising at least 30 consecutive years, a period defined by the World Meteorological Organization (WMO 2020) as the one enough to stabilize the mean and reduce the variance. Examples of phenomena considered of climate scale are El Niño–Southern Oscillation (ENSO); Madden–Julian Oscillation (MDO); Pacific Decadal Oscillation (PDO); the Atlantic Dipole (AD); Atlantic Multidecadal Oscillation (AMO); and South America Monsoon Circulation (SAMC) (Coelho et al. 2016, Cavalcanti et al. 2017; Cai et al. 2020). These phenomena are responsible for anomalies of a climatological mean value, and they can cause long-term events such as above normal droughts or rainy seasons.

The weather conditions have daily variation due to the interactions between several factors such as solar radiation, clouds, wind, and human-induced influences, mainly related to atmospheric pollution and land use (Pereira et al. 2002). Therefore, the term "climate variability" is often used to describe the deviations of meteorological conditions of a given month, season, or year in relation to their long-term statistics (climate). Climate variability can be caused by natural internal processes within the climate system, known as internal variability, or by natural or anthropogenic external factors, also called external variability (WMO 2020). Therefore, caution must be taken to avoid confusion between climate variability and climate change.

Climate change refers to a statistically significant change of the mean state of a given meteorological variable, change of its variability (tendencies), change in the frequency and intensity of extreme events (anomalies), or change in the duration of these events (decades or longer) (Alvares et al. 2021). Climate change may be caused by natural or external factors related or not to anthropogenic activities. The main possible causes of climate change are as follows: extraterrestrial, solar activity; astronomic, change in the sun-earth distance, obliquity, or precession; and terrestrial, Vulcan activity, distribution between oceans and continents, size of polar ice caps, and atmospheric composition. However, the effects of the anthropogenic and natural drivers on global climate change have been identified and simulated. The likely range of total human-caused global surface temperature increase from 1850–1900 to 2010–2019 is 0.8 to 1.3 °C, natural drivers changed global surface temperature by – 0.1 to 0.1 °C, and internal variability changed it by – 0.2 °C to 0.2 °C (IPCC 2021). Among these possible factors, the one with the most expressive changes in the last decades and expected for the next ones is the composition of the atmosphere,

expressed by the greenhouse gas (GHG) concentration. The increase of GHG emissions is primarily attributed to human activities, mainly related to burning of coal, oil and gases, deforestation, livestock, farming, and use of nitrogen fertilizers, among others. Based on that, the United Nations Framework Convention on Climate Change (UNFCCC) makes a distinction between climate change attributed to human activities that alter the atmospheric composition and the one attributed to natural causes (IPCC 2021).

Many regions around the world experience greater climate variability than others, and that depends on the climate systems that normally affect these areas. Thus, extreme events of rare occurrences, such as an intense storm associated with a tropical cyclone, a frost caused by a strong polar mass, or an intense drought in a specific area, cannot be attributed to human-induced climate change. On the contrary, an increase of air temperature over decades, showing a consistent and continuous tendency, with normal average changing by 1, 2, or 3 °C, is a clear signal of climate change or warming caused by increasing GHG concentration in the atmosphere caused by human activities. Thus, to detect climate change, researchers must rely on long-term observed meteorological data series. Long-term average and distribution of air temperatures and rainfall in a given region are key components of the general state of the climate system in that location and period of time. Therefore, a well-defined climate classification system, which can be at the same time simple, relevant, and easily replicable, is essential to detect and monitor climate change over time. Köppen climate classification system, which meets such premises, remains the most used climate classification procedure to date. Thereby, scientists have been using this classification system with success to identify climate types and track climate change at regional and global scales (Wang and Overland 2004; Rubel and Kottek, 2010, Chen and Chen 2013; Fernandez et al. 2017; Beck et al. 2018; Dubreuil et al. 2019; Cui et al. 2021). Therefore, our hypothesis is that the use of Köppen climate classification can be used to detect local climate change based on a historical series of 100 years and that such change is related to those that are occurring in other spatial scales as a consequence of increasing GHG. Considering that, the objectives of our study were to organize, consist, and make available monthly rainfall and temperature data from a centennial weather station aiming to characterize the climate variability, anomalies, and change along this period; to evaluate the influence of ENSO on climate variability; to assess the local warming caused by increasing GHG throughout the last fifty nine years; and to apply the Köppen classification system to detect climate change over 100 years of observed meteorological data in a tropical location in Southeastern Brazil.

2 Material and methods

2.1 Site study and data source

The conventional weather station (CWS) of the "Luiz de Queiroz" Agricultural College (ESALQ) of the University of São Paulo (USP) is located in the Meteorological Observatory Professor Jesus Marden dos Santos at the following geographical coordinates: 22°42′30″ South latitude and 47°38′00″ West longitude, with an altitude of 546 m above mean sea level, within a 1.5-km buffer of the rural landscape far from present urban areas (Fig. 1).

The CWS started its operations on June 1, 1902, the inaugural day of the agricultural meteorology course in the college (Dias 1917). Until 1916, only daily rainfall (R_D) was recorded. At the end of that year, a meteorological shelter was built, and in 1917, daily measurements of minimum (T_{DMIN}) and maximum (T_{DMAX}) air temperature had begun. In 1927, a heliograph was installed in the weather station for measuring the daily number of sunshine hours (h). In

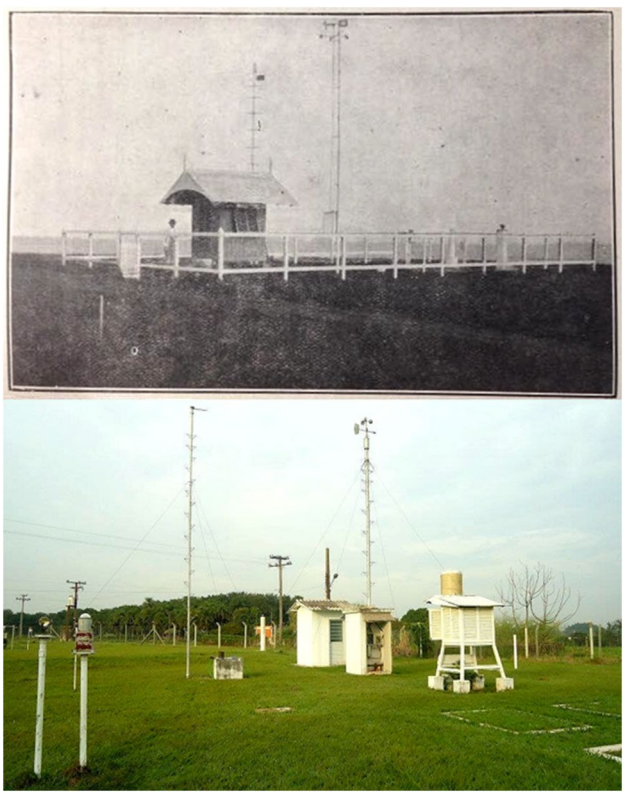

Fig. 1 Conventional weather station of the "Luiz de Queiroz" Agricultural College (ESALQ) in 1917 (picture taken by Dias 1917) (above) and in 2017 (below), in Piracicaba, state of São Paulo, Brazil

early 1943, new sensors for measuring wind speed (U_{10}) and direction at 10-m height, relative humidity (RH), Piche evaporation (Ep), and atmospheric pressure (Patm) were also installed. Later in 1978, an actinograph, which measures global solar radiation (Qg), was also set up in the CWS place layout. Lastly, in 1997, an automatic weather station (AWS) was mounted in the same area, recording all weather variables each quarter-hour (Sentelhas et al. 1997). In order to make all these observed data available for the internal and external community, since 2002 the Department of Biosystem Engineering shares all the weather datasets from the CWS and AWS through its webpage (www.leb.esalq.usp.br/leb/base.html). These continuous data series makes CWS one of the oldest weather stations in operation in the state of Sao Paulo (www.ciiagro.sp.gov.br) and in Brazil (https://mapas.inmet.gov.br).

After a century of thorough, careful, and persistent work by many ESALQ/USP employees and professors, on December 31, 2016, the CWS completed 36,524 days of uninterrupted observations of rainfall and air temperature, one of the longest data series in Brazil (Draenert 1896; Ferraz 1911, Granato 1913; Dias 1917; Morize 1927; Setzer 1946). Thus, it is with this data series that our study deals hereafter.

2.2 Data screening and processing

The CWS presents very few data gaps in R_D, T_{DMIN}, and T_{DMAX} records. R_D gaps were filled with data from AWS and from data series from rain gauges network of the DAEE. T_{DMIN} and T_{DMAX} gaps between 1997 and 2016 were filled using AWS observations, while the gaps before 1997 were filled with the Brazilian Daily Weather Gridded Data v2.1 from Xavier et al. (2016). Air temperature gaps prior to 1980 were filled using the median value calculated from the historical series for each day of the year.

Having screening and data consistency done, R_D, T_{DMIN}, and T_{DMAX} were processed for monthly resolution. Average daily air temperature (T_{DAVE}) was obtained by the arithmetic mean of T_{DMIN} and T_{DMAX}. Average monthly air temperature (T_{MAVE}) was averaged by T_{DAVE}. Lastly, average annual air temperature (T_{AAVE}) was obtained by averaging all T_{MAVE}. Daily rainfall was accumulated to have monthly rainfall (R_M) which, subsequently, was accumulated to obtain annual rainfall (R_A).

2.3 CWS data exploration and analysis

The use of data visualization techniques to make the results comprehensible and feasible is a key motivator for research and scientific communication. T_{MAVE} and R_M centennial dataset distribution were characterized by boxplot method. The whole temporal variability of T_{MAVE} and R_M were shown by filled contour plot, yearly and by 30-year moving average. T_{MAVE} and R_M anomalies were presented using heatmap plots scheme. T_{AAVE} and R_A anomalies were shown by typical bar graphs. Pearson correlations between T_{MAVE} and R_M anomalies with Niño SST indices by regions were presented in bar graphs. All evaluated anomalies treated in this paper had the period 1951–2000 as the baseline.

2.4 Climate change detection tool

In order to assess changes in the climate type observed through the CWS records, T_{MAVE} and R_M observations were averaged to obtain the climatological normals, which had two main purposes: to be a benchmark indicator against which conditions can be assessed and to be used as a pattern of weather conditions likely to occur at the studied location. The classical period of a climatological normal is comprised of 30 consecutive years, as defined by WMO. CWS climatological normals were computed for the following consecutive periods of 30 years: January 1917 to December 1946, January 1918 to December 1947, until the last one from January 1987 to December 2016, thus totaling 71 climatological normals of T_{MAVE} and R_M throughout the centennial dataset.

Köppen system criteria were applied to detect the long-term climate-type changes of CWS climatological normals. The Köppen climate types are symbolized by two or three characters, where the first indicates the climate zone and is defined by temperature and rainfall, the second considers the rainfall distribution, and the third is the seasonal temperature variation (Köppen 1936). The classification system has a total of 31 climate types divided into five zones, as shown in Table 1. We used the palette color provided by Alvares et al. (2013) to identify the climate types. These authors published a comprehensive high-resolution (100 m) study of the Köppen climate classification for Brazil.

2.5 Regional and global climate correlation analysis

The anomalies of T_{MAVE} for each month and their climatological normals were correlated with temperature anomaly datasets of three different geographic levels. The first one consisted of CRUTEM4 grid-box (5°×5°) with centroid of 22.5° South–47.5° West (Jones et al. 2012, https://crudata.uea.ac.uk) (Fig. 2), whose grid is composed of 17 weather stations described as follows: Minas Gerais State with Maria da Fé (WMO code, 830,150), São Sebastião do Paraíso (836,310), Lambari (830,320), Poços de Caldas (836,810), and Machado (836,830); São Paulo State with Votuporanga (836,230), Franca (836,300), São Simão (836,690), Catanduva (836,760), Campos do Jordão (837,140), Bauru (837,220), São Carlos (837,260), São Paulo (837,810), Taubaté (837,840), Iguapé (838,210), and Sorocaba (838,510); and Paraná State with Castro (838,130). Although the CWS

Table 1 Complete Köppen's system for climate classification

Temperature				Rainfall	Climate			Symbol
T_{COLD}	T_{HOT}	T_{AAVE}	R_M	R_A				
≥ 18 °C			$R_{DRY} \geq 60$ mm		(A) Tropical		(f) Without dry season	Af
			$R_{DRY} < 60$ mm	≥ 25 (100—R_{DRY})			(m) Monsoon	Am
				< 25 (100—R_{SDRY})			(s) With dry summer	As
				< 25 (100—R_{WDRY})			(w) With dry winter	Aw
		≥ 18 °C		≥ 5* $R_{THRESHOLD}$ & < 10*$R_{THRESHOLD}$	(B) Dry	(S) Semi-arid	(h) Low latitude and altitude	BSh
		< 18 °C					(k) Mid-latitude and high altitude	BSk
		≥ 18 °C		< 5* $R_{THRESHOLD}$		(W) Arid	(h) Low latitude and altitude	BWh
		< 18 °C					(k) Mid-latitude and high altitude	BWk
≥ − 3 °C < and < 18 °C	≥ 22		$R_{DRY} > 40$ mm		(C) Humid Subtropical	(f) Oceanic climate, without dry season	(a) With hot summer	Cfa
	< 22 °C and $T_{M10} \geq 4$						(b) With temperate summer	Cfb
≥ − 38 °C and < 18 °C	< 22 °C and $1 \leq T_{M10} < 4$						(c) With short and cool summer	Cfc
≥ − 3 °C < and < 18 °C	≥ 22 °C		$R_{DRY} < 40$ mm $R_{SWET} \geq 10 * R_{WDRY}$			(w) With dry winter	(a) And hot summer	Cwa
	< 22 °C and $T_{M10} \geq 4$						(b) And temperate summer	Cwb
≥ − 38 °C and < 18 °C	< 22 °C and $1 \leq T_{M10} < 4$						(c) And short and cool summer	Cwc
≥ − 3 °C < and < 18 °C	≥ 22 °C		$R_{DRY} < 40$ mm $R_{WWET} \geq 3 * R_{SDRY}$ $R_{SWET} < 10 * R_{WDRY}$			(s) With dry summer	(a) And hot	Csa
	< 22 °C and $T_{M10} \geq 4$						(b) And temperate	Csb
≥ − 38 °C and < 18 °C	< 22 °C and $1 \leq T_{M10} < 4$						(c) And short and cool summer	Csc
≥ − 38 °C and < − 3 °C	≥ 22 °C		$R_{DRY} > 40$ mm		(D) Temperate continental	(f) Without dry season	(a) With hot summer	Dfa
	< 22 °C and $T_{M10} \geq 4$						(b) With temperate summer	Dfb
	< 22 °C and $1 \leq T_{M10} < 4$						(c) With short and cool summer	Dfc
< − 38 °C and < − 3 °C							(d) With very cold winter	Dfd
≥ − 38 °C and < − 3 °C	≥ 22 °C		$R_{DRY} < 40$ mm $R_{SWET} \geq 10 * R_{WDRY}$			(w) With dry winter	(a) With hot summer	Dwa
	< 22 °C and $T_{M10} \geq 4$						(b) And temperate summer	Dwb
	< 22 °C and $1 \leq T_{M10} < 4$						(c) And short and cool summer	Dwc
< − 38 °C and < − 3 °C							(d) And very cold winter	Dwd
≥ − 38 °C and < − 3 °C	≥ 22 °C		$R_{DRY} < 40$ mm $R_{WWET} \geq 3 * R_{SDRY}$ $R_{SWET} < 10 * R_{WDRY}$			(s) With dry summer	(a) And hot	Dsa
	< 22 °C and $T_{M10} \geq 4$						(b) and temperate	Dsb
	< 22 °C and $1 \leq T_{M10} < 4$						(c) And short and cool summer	Dsc
< − 38 °C and < − 3 °C							(d) And very cold winter	Dsd
	< 10 and ≥ 0 °C				(E) Polar	(T) Tundra		ET
	< 0 °C					(F) Frost		EF

T_{COLD} average air temperature of the coldest month; T_{HOT} average air temperature of the hottest month; T_{AAVE} annual average air temperature; R_M monthly rainfall; R_A annual rainfall; R_{DRY} average rainfall of the driest month; R_{SDRY} average rainfall of the driest month in summer; R_{WDRY} average rainfall of the driest month in winter; R_{SWET} average rainfall of the wettest month in summer; R_{WWET} average rainfall of the wettest month in winter; T_{M10} number of months where the temperature is above 10 °C; $R_{THRESHOLD} = 2(T_{AAVE})$, if at least 70% of R_A occurs in winter; $R_{THRESHOLD} = 2(T_{AAVE}) + 28$, if at least 70% of R_A occurs in summer, and $R_{THRESHOLD} = 2(T_{AAVE}) + 14$, otherwise; for the Southern Hemisphere, summer is defined as the warmer 6-month period (ONDJFM) and winter is defined as the cooler 6-month period (AMJJAS). For the Northern Hemisphere, summer is defined as the warmest 6-month period (AMJJAS) and winter is defined as the coolest 6-month period (ONDJFM)

is located within the grid-box, its data was not used by Jones et al. (2012), making it genuinely independent data (Fig. 3). The second and third levels are from NOAA time series (www.ncdc.noaa.gov/cag/time-series) here represented, respectively, by South America and Global. Both land temperature anomalies came from the Global Historical Climatology Network-Monthly (GHCN-M) dataset in their fourth release (Menne et al. 2018).

We also evaluated the long-term CWS climate with El Niño–Southern Oscillation (ENSO) observations (https://psl.noaa.gov/gcos_wgsp/Timeseries) in order to investigate the correlations between T_{MAVE} and R_M and the four Niño Sea Surface Temperature (SST) index regions: Niño 1 + 2 (0-10S, 90 W-80 W); Niño 3 (5 N-5S, 150 W-90 W), Niño 3.4 (5 N-5S, 170 W-120 W), and Niño 4 (5 N-5S, 160E-150 W) (Fig. 2). For correlation analyzes, T_{MAVE} and R_M anomalies of each month and their climatological normals were considered.

Finally, the relationship between continental and global annual temperature anomalies against the long-term carbon dioxide (CO_2) concentrations in the Earth's atmosphere was also investigated by considering the climatological normal from 1958–1987 to 1987–2016. Also, we added two other air temperature datasets to assess the concordance between local and regional temperatures and CO_2 levels. All these air temperature datasets already were described previously, as follows: at local level were used the CWS air temperature (T_{AAVE}), at regional level were used the annual temperature anomalies of CRUTEM4 grid-box (22.5° South–47.5° West), at continental level were used the land temperature anomalies of South America, and at global level were used the land temperature anomalies of all Globe. Long-term CO_2 concentrations from 1958 to 2016 were obtained from NOAA Lab in Mauna Loa, Hawaii, USA (www.esrl.noaa.gov/gmd/ccgg), from 1958 until 2016, matching with CWS temperature dataset for the same period.

3 Results and discussion

January was the wettest month with R_M averaging 227 mm, and maximum and minimum R_M of 491 mm and 61 mm, respectively (Fig. 4). Both July and August were the driest months with R_M averaging 29 mm. February was the warmest month with average T_{MAVE} of 24.8 °C, with observations ranging between 22.6 and 27.7 °C. T_{MAVE} observations showed July as the coldest month with average, minimum, and maximum values of 17.6, 14.9, and 19.8 °C, respectively. The monthly distribution shows the highest climate variability from late spring to summer for R_M (November to March, with standard deviation (σ) > 60 mm), and in the opposite seasons, early fall to late spring, for T_{MAVE} (April to October, with σ greater than 1 °C). The rainiest months (R_M > 300 mm) occurred 51 times in 41 years, mainly in January (23% of the years), February (11%), December (11%), and May (1%). In 1983, annual rainfall of 2022 mm was recorded at the CWS, representing the wettest year for the investigated period (Figs. 5 and 7). Driest months (R_M < 40 mm) have been observed at least once a year, however, being more common to have this condition from 3 to 5 months per year (usually from May to September). These climatic traits are typical of Southeastern Brazil, which has a wet and hot summer and a dry and mild winter (Alvares et al. 2013). Frost days are usually quite rare in the study area (Alvares et al. 2018).

CWS observations presented an T_{AAVE} of 21.7 °C (σ = 0.7 °C) for the entire period studied. T_{MAVE} showed a substantial interannual variability, with T_{AAVE} increasing throughout the 100 years (Fig. 5 and 7). Figure 5 contains 2400 months of data (half for T_{MAVE} and half for R_M) into a unique visualization. T_{MAVE} below 16 °C were observed until 1988. Low winter temperatures were more frequent at the beginning of the series (between 1917 and 1925) but also occurring approximately every 10 years after that (1939–1942, 1951–1953, 1962–1964, 1976–1981). Freezing winters (T_{MAVE} < 16 °C) were mostly observed in July (12% of the years), June (4%), and May (1%). Likewise, May 1972 was the last month of the most remarkable negative anomaly (− 3.8 °C). After the mid-1980s, the T_{MAVE} heatmap showed mainly reddish colors, noted by positive anomalies of temperature indicating the starting of the striking warming period (Fig. 6). Moreover, a major trend of positive T_{AAVE} anomaly is observed over the past 35 years (Fig. 7), with the anomaly increasing at a rate of about 0.032 °C year^{-1} (R^2 = 0.39, p < 0.01). These results converge with the performed analysis by Geirinhas et al. (2018), which revealed the existence of positive and significant trends in heat waves frequency since the 1980s in Southeastern Brazil. Furthermore, in all the Brazilian regions, the frequency of heat waves increased, whereas the frequency of cold waves decreased between 1961 and 2016 (Bitencourt et al. 2020).

Very hot summer (T_{MAVE} > 26 °C) was firstly observed in December 1940 in the CWS data series. After that, it was also observed in January 1956, and then in February 1977 (Fig. 5). From this time onwards, an expressive increase of very hot summer months, with T_{MAVE} > 26 °C, was detected in two months in the 1980s, three months in the 1990s, four months in the 2000s, and twelve months from 2011 to 2016. In the 2010s, T_{MAVE} > 26 °C happened for three consecutive months (Dec/Jan/Feb) in the summers of 2013/2014, 2014/2015, and 2015/2016, resulting in mega heat wave episodes (Figs. 5 and 6). Very hot summers were most frequent in February (11% of the years), January (7%), December (4%), and October (1%). All months of 2015 showed positive

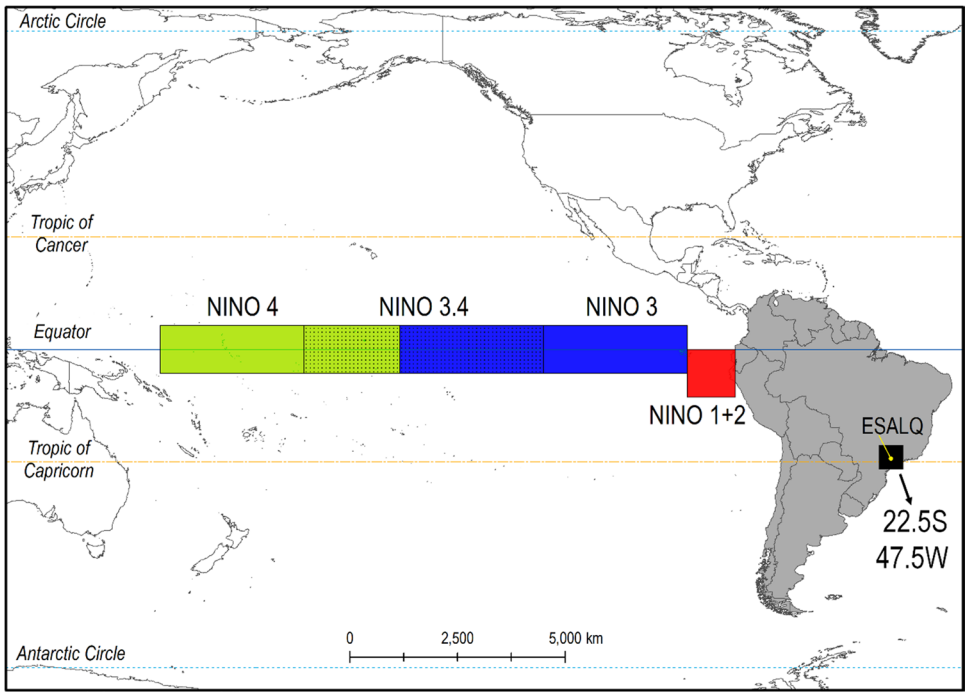

Fig. 2 Niño sea surface temperature (SST) indices regions (Niño 1 + 2 = 0-10S, 90 W-80 W, red region; Niño 3 = 5 N-5S, 150 W-90 W, blue region; Niño 3.4 = 5 N-5S, 170 W-120 W, dotted green and blue region; and Niño 4 = 5 N-5S, 160E-150 W, green region). South America is highlighted in gray, black square is the CRUTEM4 22.5S 47.5 W grid-box, and the yellow dot is the ESALQ's conventional weather station, located in Piracicaba, state of São Paulo, Brazil (22°42′30″S and 47°38′00″W)

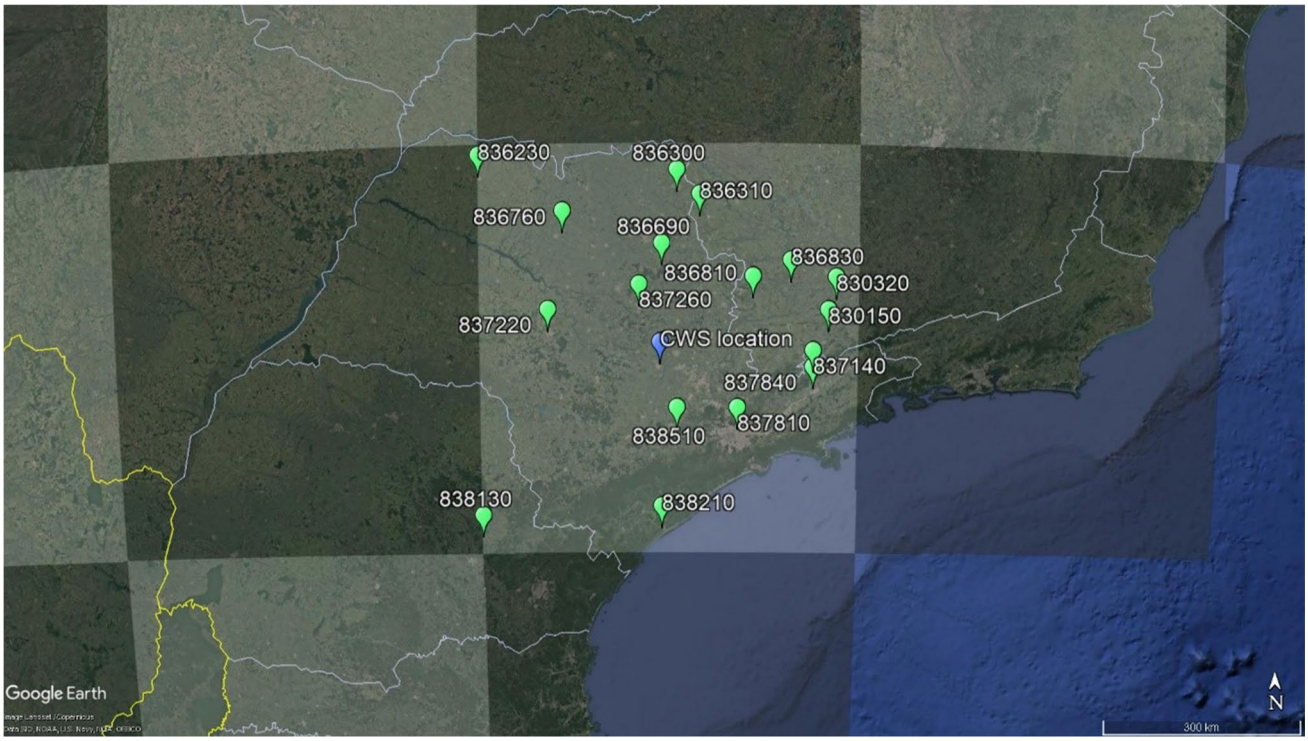

Fig. 3 CRUTEM4 grid box (centroid in 22.5° South–47.5° West, Jones et al. 2012, https://crudata.uea.ac.uk) in light gray at center of the map and the 17 weather stations used to represent it in green markers: Maria da Fé (WMO code, 830,150), São Sebastião do Paraíso (836,310), Lambari (830,320), Poços de Caldas (836,810), Machado (836,830), Votuporanga (836,230), Franca (836,300), São Simão (836,690), Catanduva (836,760), Campos do Jordão (837,140), Bauru (837,220), São Carlos (837,260), São Paulo (837,810), Taubaté (837,840), Iguapé (838,210), Sorocaba (838,510), and Castro (838,130). ESALQ's conventional weather station, located in Piracicaba, state of São Paulo, Brazil, is the blue marker in the map

anomalies, and January was the hottest month of all CWS series with T_{MAVE} of 27.7 °C (Figs. 5 and 6).

The historical average annual rainfall (R_A) for Piracicaba was 1279 mm, with $\sigma = 218$ mm, which represents, approximately, 17% of interannual variability. There is at least a 90% probability (10th percentile) that R_A will be equal to or exceed 984 mm. An 80% probability (20th percentile) is expected for R_A above 1091 mm, which is a critical threshold for identifying a severe meteorological drought. Seventeen years presented annual rainfall below ($R_A - \sigma$). However, the occurrence of two or more consecutive years of annual rainfall below the critical level constitutes severe periods of water scarcity. Five pairs of consecutive years with critical rainfall conditions were observed in the historical weather series: 1924–1925; 1963–1964; 1968–1969; 1978–1979; and 1984–1985. Notice that years or periods with strong negative R_A anomalies are commonly associated with positive T_{AAVE} anomalies (Fig. 7). These anomalies are likely associated with anticyclonic systems promoted by anomalous westward displacements of the South Atlantic Subtropical High System which are related to a weakening of other transitional systems such as the ITCZ and the SACZ (Geirinhas et al. 2018). These strong negative R_A anomalies associated with positive T_{AAVE} anomalies, as observed in the last years at Piracicaba, is compatible with an increase in solar radiative pattern and decreased soil moisture, which enhances surface temperature values, possibly associated with positive feedback mechanisms between the surface and the atmosphere (Geirinhas et al. 2018).

The last 6 years of the CWS weather series were totally abnormal since intense heat waves resulted in extensive dry spells. The austral summer seasons of 2013/2014 and 2014/2015 was characterized by extraordinary concurrent drought and heatwave conditions stemmed by severe rainfall deficits and a higher-than-average occurrence of atmospheric blocking patterns (Geirinhas et al. 2021). In those periods, the heat waves associated with low or no rainfall in August and September have made this time of the year, which represents the transition from the late winter to early spring, in a persistent sequence of consecutive days of extremely hot and dry conditions, triggering severe meteorological droughts, crop yield losses, increase in forest fire hazard, and drastic water rationing for human, industry, and agriculture uses. By January 2015, main reservoirs in the Piracicaba River basin had reached storage levels of only 5% of their 1.3 billion m^3 capacity (Nobre et al. 2016). This dramatic situation of two consecutive years with heat waves and drought (2014/2015) was tackled in almost all municipalities of São Paulo state and by water management authorities to avoid social chaos during an atypical water shortage in a region that is home to more than 40 million people (Seth et al. 2015; Braga and Kelman 2020). Another major latent concern is the lack of power grid supply infrastructure face to the potential

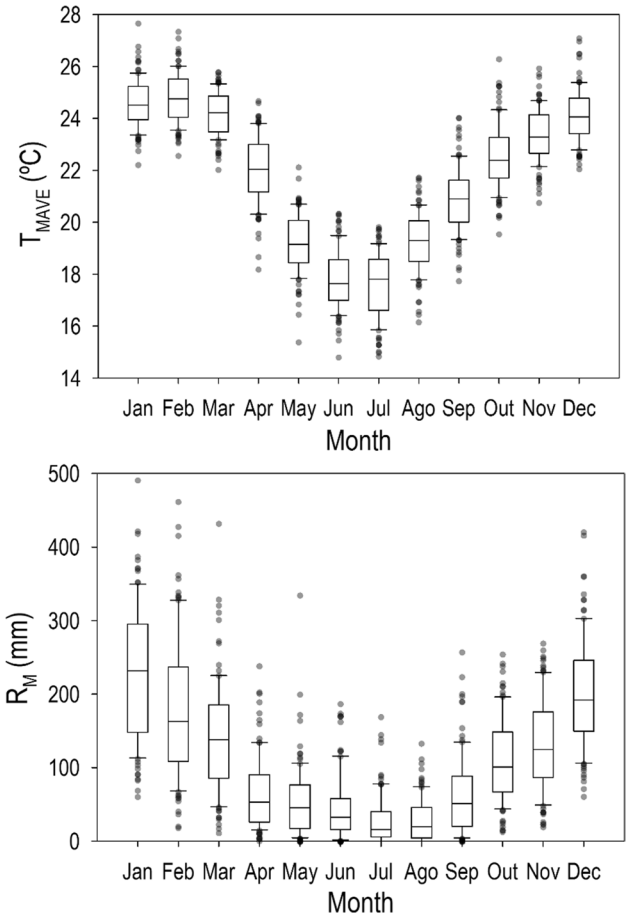

Fig. 4 Monthly variability of average air temperature (T_{MAVE}) (above) and rainfall (R_M) (below) between 1917 and 2016 in the ESALQ's conventional weather station, located in Piracicaba, state of São Paulo, Brazil

increase of 326% in the air conditioning energy consumption related to expected air warming up to 4 °C in Southeastern Brazil in next coming years (Bezerra et al. 2021). Our results reveal a substantial contribution of persistent dry conditions to heat wave episodes, highlighting the vulnerability of the region to the power supply in the face of climate change.

Climatological normal and filled contour plot are together a very suitable and capable tool for showing climate data trends. All months presented a clear trend of rising T_{MAVE} throughout 30-year moving averages. January, July, August, October, November, and December had a T_{MAVE} linear positive trend for all studied periods, with R^2 of 0.75, 0.87, 0.81, 0.91, 0.88, and 0.70, respectively (data not shown). February, March, April, May, and June showed a negative linear trend early in the twentieth century. However, only after the 1950s an apparent temperature increase is observed, revealing a positive linear trend (R^2 of 0.96, 0.98, 0.98, 0.89, and 0.94, respectively). September was an abnormal month with temperature showing a strong positive trend from 1917–1946

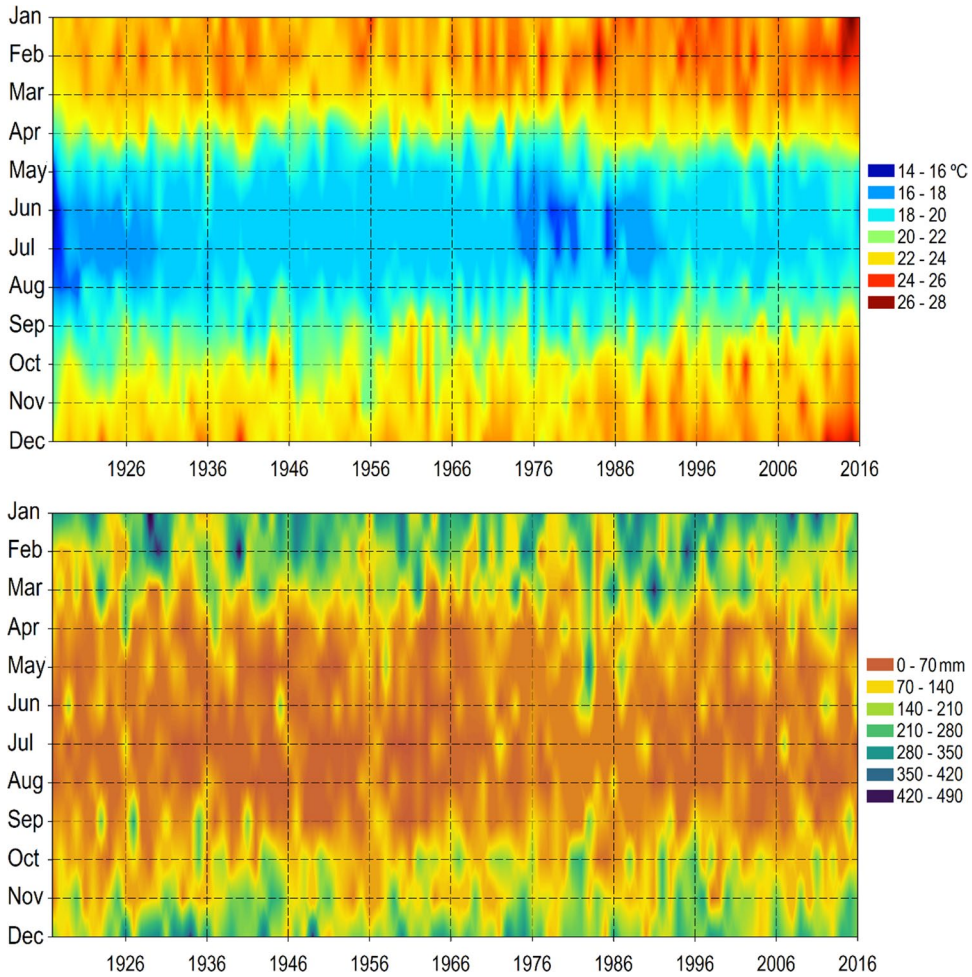

Fig. 5 Temporal variability of the monthly average air temperature (T_{MAVE}) (above) and rainfall (R_M) (below) between 1917 and 2016 in the ESALQ's conventional weather station, located in Piracicaba, state of São Paulo, Brazil

to 1946–1975, a negative trend (cooling) in the sequence until 1964–1993 and again a strong positive trend until the end of the assessed period. Notice that the bluish color started to fade and narrow from the 1970s in filled contour plot (Fig. 5). Hence, stronger red colors begin to appear after that period for January and March, and more recently, for December too. Still analyzing the 30-year moving averages, a negative trend for R_M for February and December (R^2 of 0.53 and 0.69) were found. For these two months, a negative correlation ($p < 0.01$) between R_M and T_{MAVE} were found (Fig. 8). January, September, and November did not present any rainfall trend for the assessed period, which is the opposite to what was observed for March, April, May, June, July, August, and October, which presented positive rainfall trends ($p < 0.01$), with R^2 of 0.54, 0.65, 0.86, 0.25, 0.71, 0.33, and 0.28 respectively. Most of these months (early fall to late winter) showed negative correlations ($p < 0.01$) between R_M and T_{MAVE} (Fig. 8).

T_{AAVE} increased 0.9 °C over the 100 years, rising from 21.4 °C for the first climatological normal (1917–1946) to 22.3 °C for the last one (1987–2016) (Fig. 9). Between 1917–1946 and 1951–1980, the T_{AAVE} floated around 21.4 °C; however, henceforth 1952–1981, a constant increase in T_{AAVE} was observed, with an approximate mean rate of 0.0249 °C 30-year moving average^{-1}. The average air temperature of the hottest month (T_{HOT}) rose from 24.5 to 25.3 °C during the analyzed period and had a slower warming increment of 0.0214 °C 30-year moving average^{-1} after the period 1952–1981. Winter months (T_{COLD}) had the highest temperature increase, rising from 17.1 (1917–1946) to 18.3 °C (1987–2016), which represents a mean rate of 0.0259 °C 30-year moving average^{-1} (Fig. 9).

Three major trends in annual rainfall over the 30-year moving average were observed throughout along the CWS historical series. From 1917–1946 to 1922–1951, R_A had an increase from 1250 to 1300 mm. After that, a reduction to 1205 mm was observed until 1951–1980. From then, another period of R_A increase was observed, reaching 1350 mm in the last period of the climatological normal (1987–2016) (Fig. 9). The percentage of summer rainfall (R_{SUMMER}) in relation to R_A dropped substantially from 82% in 1939–1968 to 75% from 1963–1992 onwards; however, the rainfall of the wettest month in the summer (R_{SWET}) remained constant, whereas the rainfall of the driest month in winter (R_{WDRY})

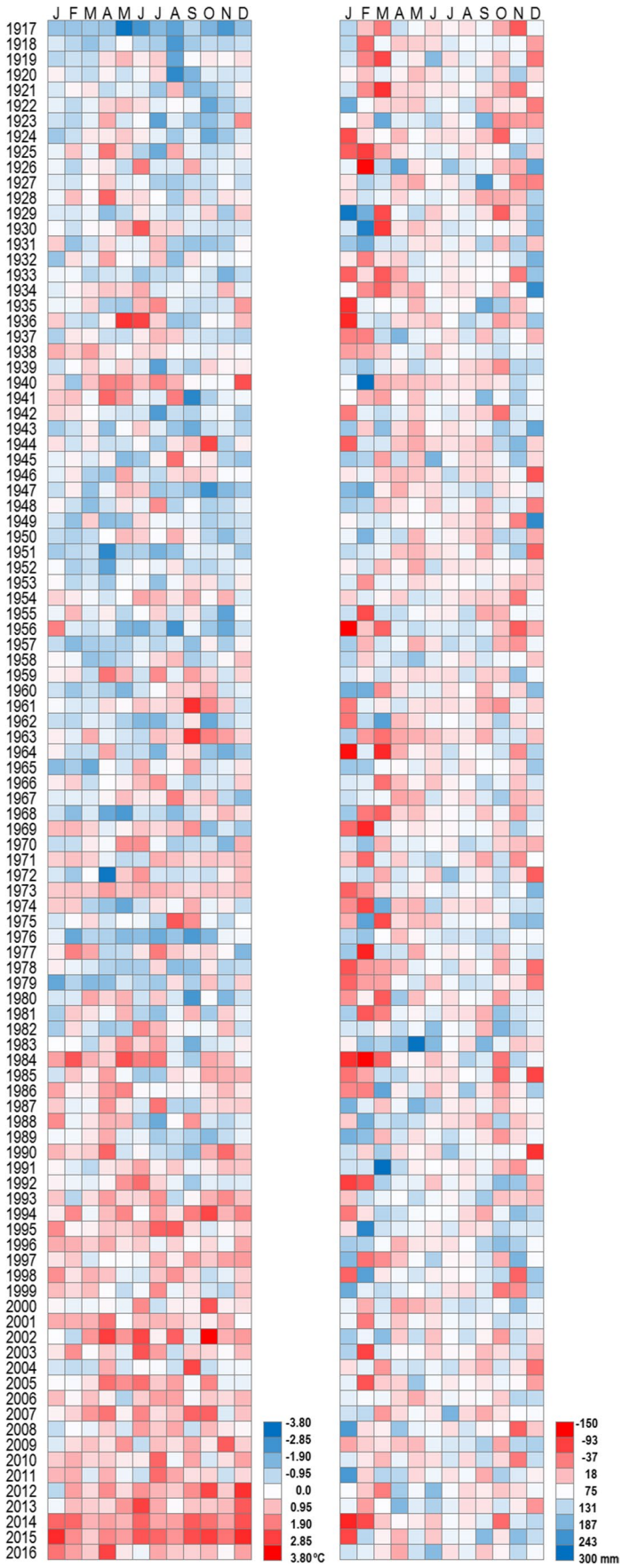

Fig. 6 Monthly climate anomalies between 1917 and 2016, in the ESALQ's conventional weather station, located in Piracicaba, state of São Paulo, Brazil: Left, anomaly of monthly average air temperature (T_{MAVE}); right, anomaly of monthly rainfall (R_M). The anomalies were calculated considering 1951–2000 as the baseline period

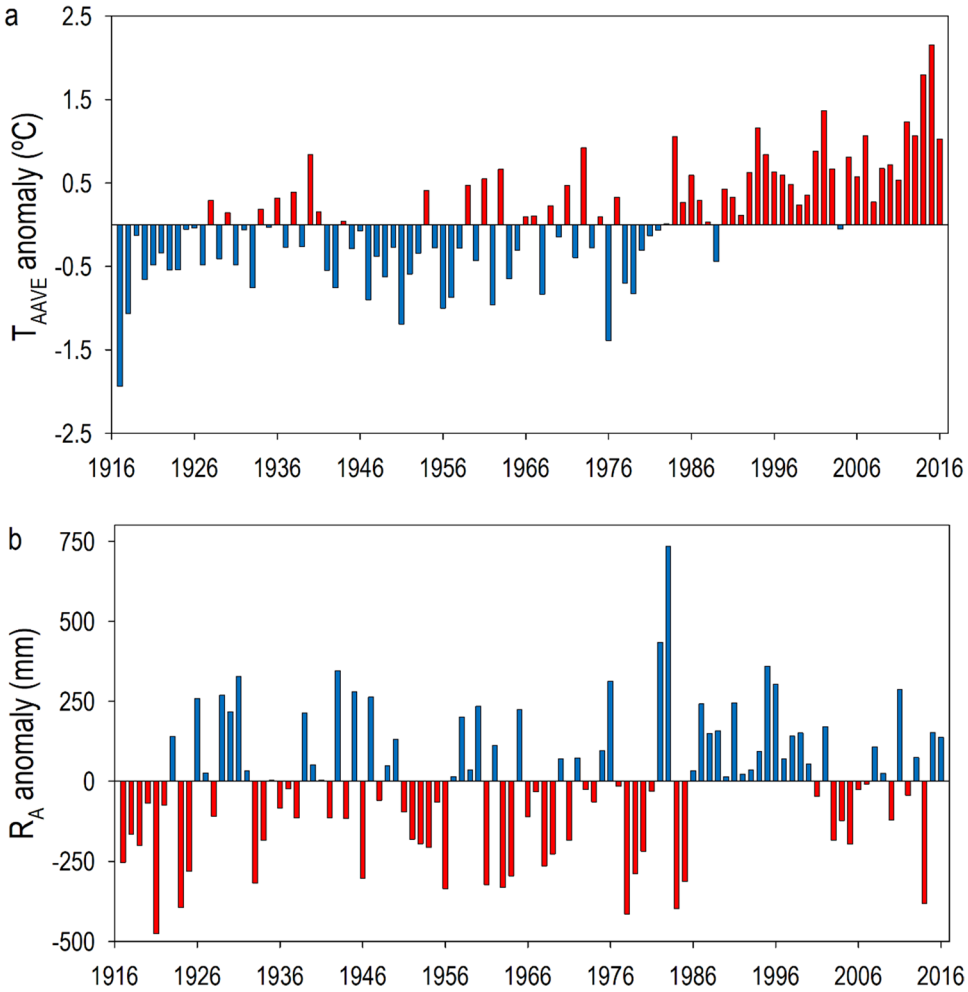

Fig. 7 Annual climatic anomalies between 1917 and 2016, in the ESALQ's conventional weather station, located in Piracicaba, state of São Paulo, Brazil: **a** anomaly of annual air temperature (T_{AAVE}); **b** anomaly of annual rainfall (R_A). The anomalies were calculated considering 1951–2000 as the baseline period

increased, mainly after 1941–1970 (Fig. 9). Marengo et al. (2020) also found a positive trend in annual precipitation between 1930 and 2019 for the metropolitan area of São Paulo, about 150 km from Piracicaba, but mainly due to an increase in the frequency of extreme precipitation events, and an increasing number of consecutive dry days, indicating an important climate change in recent times based on slightly moving and intensified of the South Atlantic Subtropical Anticyclone for southwestward of its normal position.

Subtropical conditions at the CWS located in Piracicaba persisted from the beginning of our analysis (1917–1946) until the climatological normal of 1979–2008. After this period, the climatological normals from 1980–2009 to 1987–2016 showed a change in the climate type of Piracicaba, which changed from subtropical (C) to tropical (A) conditions (Fig. 9), showing a clear tendency of tropicalization. Most of the assessed period was classified as a humid subtropical without dry season with hot summer (Cfa climate type). Of the 71 climatological normals, 55 were classified as Cfa, eight as humid subtropical with dry winter and hot summer (Cwa climate type), and the last eight as tropical with dry winter (Aw climate type). Note that both the rainfall distribution criteria ($R_{DRY} < 40$ mm, $R_{SWET} \geq 10 * R_{WDRY}$) were complied in the last climatological normal (1987–2016), which would result in a Cwa climate type. However, the air temperature of the coldest month ($T_{COLD} \geq 18$ °C) must be fulfilled first, classifying it with the tropical climate (Alvares et al. 2013). Granato (1913), Morize (1927), and Setzer (1946) also identified Piracicaba as Cwa climate type in the early twentieth century.

The $T_{COLD} \geq 18$ °C trigger is a Köppen's elementary rule that discriminates tropical climates from the other types, such as subtropical, temperate, and semi-arid (Table 1). Warmer winter conditions began to become more frequent from the 1980s and later on. In this decade, three years with $T_{COLD} \geq 18$ °C were recorded, whereas in the 1990s were three years and in the 2000s were nine, with four of them occurring sequentially, from 2012 to 2015 (Fig. 6). These accumulated warmer winters observed particularly in the last 40 years resulted in $T_{COLD} \geq 18$ °C for the last eight

climatological normals (from 1980–2009 to 1987–2016), forcing to a tropicalization of the climate of the assessed region (Fig. 9).

A similar tropicalization process was also observed for Franca (20°35′00″ South latitude and 47°22′00″ West longitude, with an altitude of 1026 m above mean sea level), in the state of São Paulo. In the last 80 years (1931–2010), the subtropical climate of this site, located about 250 km from Piracicaba, has changed to a typical tropical pattern. Franca is placed northern Piracicaba and within the CRUTEM4 22.5S 47.5 W grid-box studied (Fig. 3). During the first available climatological normal of Franca (1931–1960), R_A of 1499 mm, T_{AAVE} of 20 °C, T_{COLD} of 17.3 °C, and T_{HOT} of 21.6 °C were observed (Brasil 1970). These climatic traits were classified as a humid subtropical with dry winter and temperate summer (Cwb climate type), as also found by Granato (1913), Morize (1927), and Setzer (1946) for the same period. The following climatological normal (1961–1990) showed that Franca became warmer with an observed T_{AAVE} of 20.5 °C, T_{COLD} of 17.7 °C, T_{HOT} of 22 °C for summer months (January and February), and with R_A of 1643 mm (Ramos et al. 2009). Higher temperatures in the winter and mainly in the summer changed Franca's climate type to humid subtropical with dry winter and hot summer (Cwa climate type). Between 1981 and 2010, the last official Brazilian climatological normal, Diniz et al. (2018) showed that in Franca the temperature rose compared to the previous standard period: T_{AAVE} of 20.9 °C, T_{COLD} of 18.2 °C, and T_{HOT} of 22.4 °C for the consecutive six months (October–March), R_A of 1673 mm, and R_{DRY} of 18 mm. Hence, applying the Köppen criteria (Table 1) to those data, Franca's climate type has been changed to tropical with dry winter (Aw). Both Franca and Piracicaba have increased the T_{AAVE} by 0.9 °C over almost a century of observed data. Our findings converge with Dubreuil et al. (2018), which have identified an intensification of the tropicalization of climates in vast areas of the Brazilian territory by applying an annual climate type approach. These authors using a discretized mapping of climate change showed that tropical climate domains moved towards higher latitudes and altitudes of southern Brazil, including the present study area. Global climate modelling also detected an intense tropicalization of the inland southeastern Brazil between last century climate (Peel et al. 2007) and climatological normal of present day (1980–2016) exhibited by Beck et al. (2018), with study area shifting from Cfa to Aw climate type, as observed by us.

As expected, the average air temperature anomalies showed increasing in Pearson's correlation coefficient levels according to different observation scales: CRUTEM4 22.5S-47.5 W grid-box > South America > Global (Fig. 10a). Coefficients of correlation between Piracicaba and the Global temperature anomalies were between 0.3 and 0.5 (all with $p < 0.001$). For the South America level, the monthly coefficients of correlation varied between 0.4 and 0.62. The

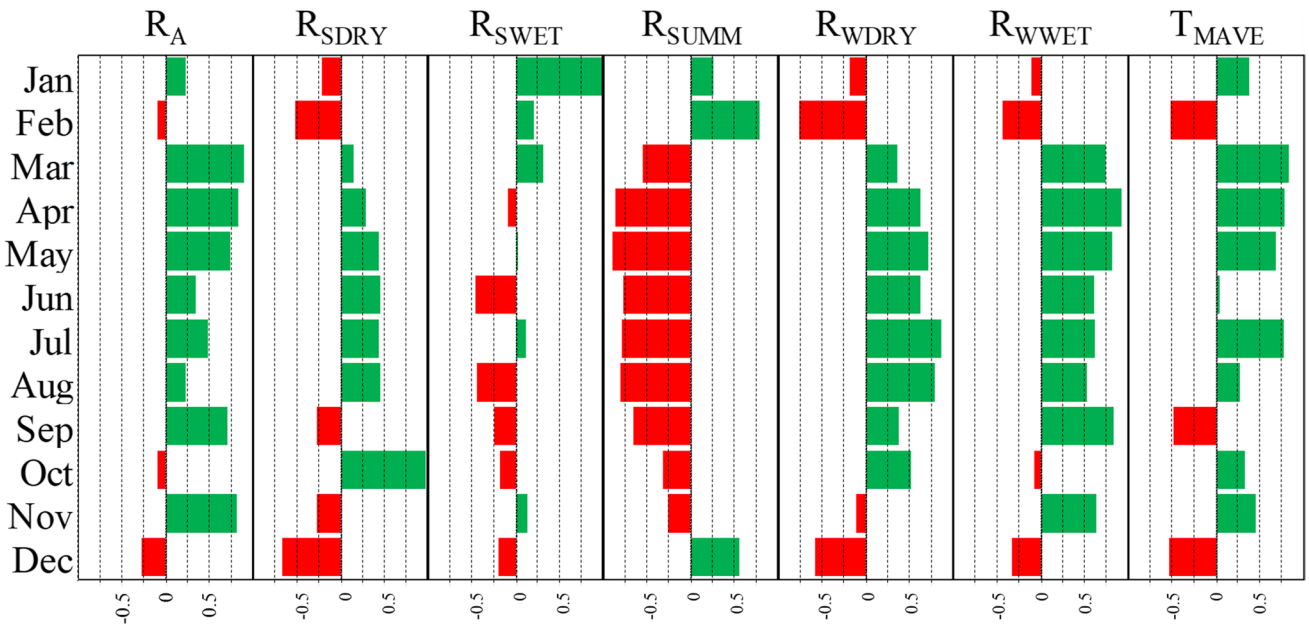

Fig. 8 Pearson correlation coefficient between R_M (monthly rainfall) and the following variables: R_A (annual rainfall); R_{SDRY} (average rainfall of the driest month in summer); R_{SWET} (average rainfall of the wettest month in summer); R_{WDRY} (average rainfall of the driest month in winter); R_{SUMM} (percentage of summer rainfall); R_{WWET} (average rainfall of the wettest month in winter); and T_{MAVE} (monthly average air temperature), considering the 30-year moving averages of the ESALQ's conventional weather station, located in Piracicaba, state of São Paulo, Brazil

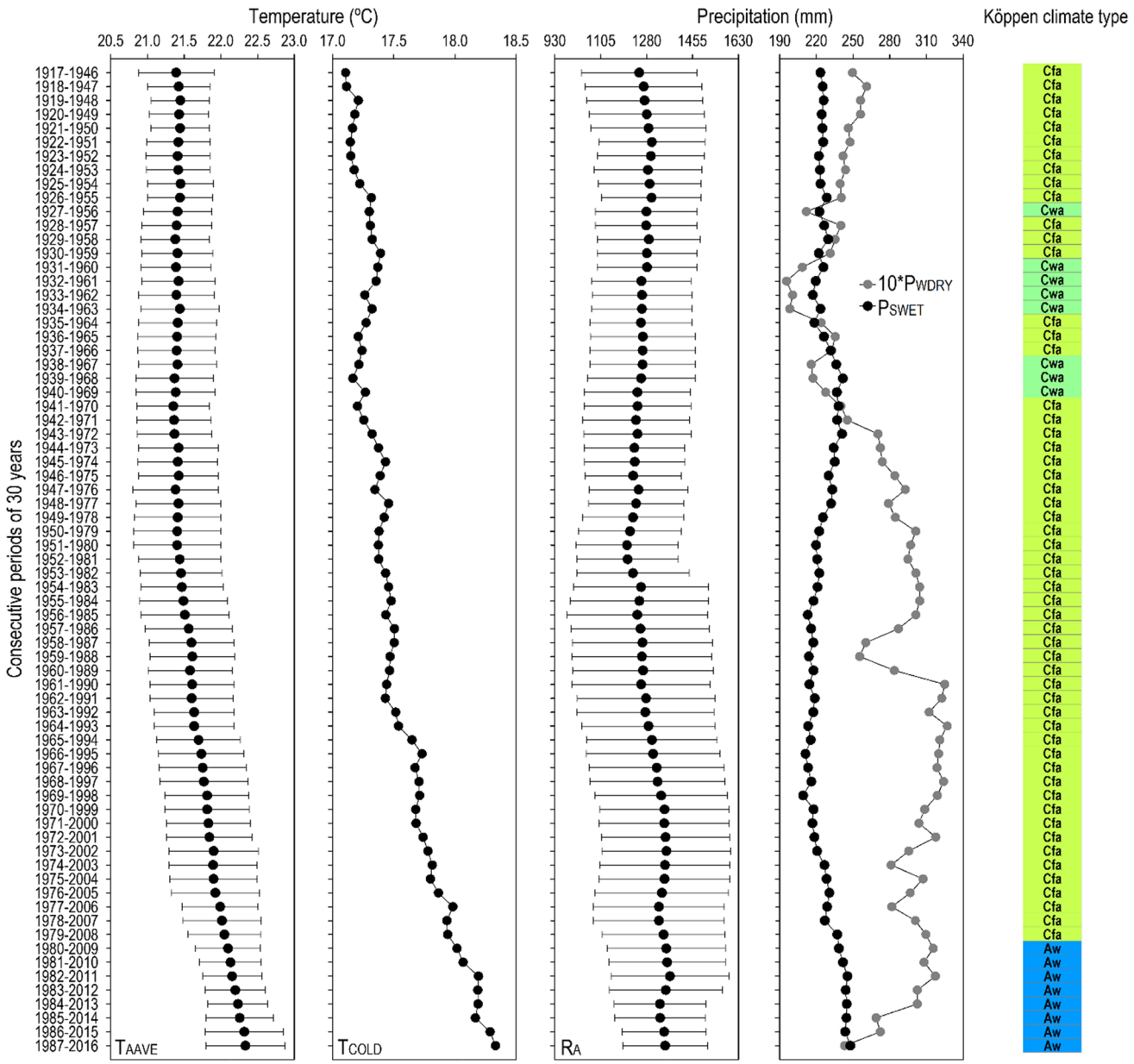

Fig. 9 Long-term climate trends, Köppen indices, and Köppen climate classification for the period between 1917 and 2016 in the ESALQ's conventional weather station, located in Piracicaba, state of São Paulo, Brazil: T_{AAVE} = annual average air temperature (°C); T_{COLD} = average air temperature of the coldest month; R_A = annual rainfall; R_{WDRY} = average rainfall of the driest month in winter; R_{SWET} = average rainfall of the wettest month in summer. Bars represent the standard deviation for T_{AAVE} and R_A

monthly correlation between Piracicaba and the 17 weather stations found within the CRUTEM4 22.5S 47.5 W grid-box revealed Pearson's correlation coefficients varying 0.78 and 0.88. Regarding the 30-year moving average comparisons, higher level of correlation for temperature anomalies for the Global and South America observations were obtained, sometimes exceeding the correlation found in the most localized comparison (Fig. 10b). These findings denote that local warming is closely related to the increase in temperature on South America and Global scales.

T_{MAVE} anomalies correlate better with the SST Niño 4 region, both annually and 30-year moving average (Fig. 11). Niño 1 + 2 region showed a greater correlation with T_{MAVE} anomalies in the summer months. Overall, the regions Niño 3, Niño 4, and Niño 3.4 had a high correlation with temperature anomalies (30-year moving average) in most months in Piracicaba. Curiously, September's T_{MAVE} was negatively correlated with the Niño 1 + 2 region, and no other correlation with other SST Niño regions were observed for this month (Fig. 11b). For R_M anomaly analysis, the correlations

with the SST Niño regions were weaker; however, important key signs were found. Positive correlations from March to November were observed for most of the months for both time scales (yearly and 30-year moving average). In early summer (December and January), the correlations turned out for the negative field and no-pattern for SST Niño regions was observed (Fig. 12). The rainfall deficit over southeast Brazil was also identified as positively correlated with the warm SST over the equatorial western Pacific Ocean and negatively correlated with the equatorial central Pacific Ocean by Coelho et al. (2016) and Cavalcanti et al. (2017). El Niño events warming pattern inhibits the southwards migration of the rain-bearing Atlantic ITCZ, commonly resulting in negative rainfall anomalies in northeast Brazil and the Amazon basin (Cai et al. 2020). Reciprocally, La Niña events tend to generate cold SST anomalies in the tropical North Atlantic region, reinforcing the southwards shift of the ITCZ and bringing anomalously high rainfall to northern South America. Oliveira Souza et al. (2018) surveying the spectral trends of vegetation with rainfall in events of El Niño-Southern Oscillation found the Atlantic Forest biome responds better to El Niño events, which results in a greater correlation with rainiest years in those regions.

We found absolute long-term linear relationships ($R^2 = 0.99$; $p < 0.001$) between continental and global annual temperature anomalies and CO_2 air concentration observed at the NOAA Lab in Mauna Loa, in Hawaii (Fig. 13). These findings show that the observed increases in air temperature are certainly related to the increase in CO_2 concentration in large-scale geographic levels. CO_2 is the most common GHG emitted by human activities, and this is contributing to the long-term trend of rising global temperatures (IPCC 2021). Both relationships presented in Fig. 13 corroborate the statements of the sixth Assessment Report (AR6) that reaffirmed with high confidence the AR5 finding that there is a near-linear relationship

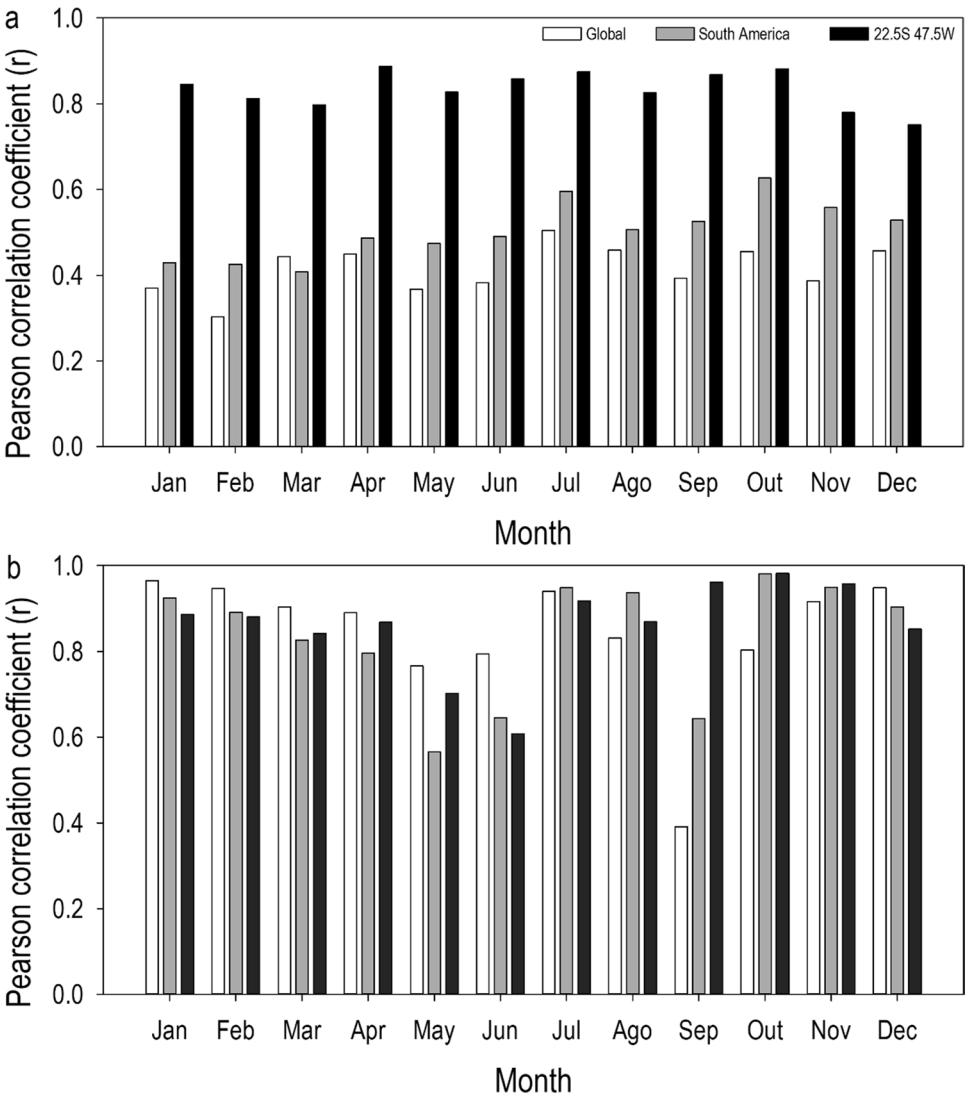

Fig. 10 Coefficient of correlation of average air temperature anomalies (baseline period: 1951–2000) between ESALQ's conventional weather station (CWS) and Global and South America Land (NOAA time series), and the CRUTEM4 22.5S 47.5 W grid-box (Jones et al. 2012): **a** observed average monthly air temperature (T_{MAVE}); **b** 30-year moving average (1917–2016)

between cumulative anthropogenic CO_2 emissions and the global warming they cause (IPCC 2021). Figure 13 also shows that there is concordance between local and regional temperatures and CO_2 levels. Analytically, in the climatological normal of 1958–1987, the average annual air temperature (T_{AAVE}) at Piracicaba was 21.6 °C for an average CO_2 level in the Earth's atmosphere about of 330 ppm. For the last evaluated climatological normal (1987–2016), the average CO_2 air concentration was 374 ppm for a hotter Piracicaba, reaching an average air temperature of 22.3 °C. In the early analyzed years, 1958–1987 to 1965–1994, T_{AAVE} rate was 0.0137 °C for a CO_2 rate of 1.25 ppm in each 30-year moving average. In the last seven climatological normals (1981–2010/1987–2016) T_{AAVE} rate rose 0.0338 °C for a CO_2 rate of 1.78 ppm. Considering the analyzed time series of 59 years, our findings show air warming of about 0.0174 °C for each 30-year moving average (Fig. 13). These results may evidence a significant anthropogenic-induced warming on a local scale, also suggesting that human-induced climate change (by GHG emissions, land use changes, per example) is becoming very apparent in the last years. Abreu et al. (2019) observed a trend of 1.1 °C per 50-year in Southeast Brazilian temperatures attributing these changes to the increasing greenhouse gas emissions. These authors calculated a trend of 0.19 to 0.30 °C per decade due to GHG, with a small contribution from other anthropogenic factors, of − 0.07 to 0.01 °C per decade. However, adding local and global trends in temperature increases shows that the question of scale is fundamental here. In the IPCC's AR6 report, there are regions in the world that are warming up faster than others (in the Arctic, per example); there would therefore be a poor correlation between rising temperatures and CO_2 levels. On the other hand, other locals much less numerous, where the temperature changes little or even decreases slightly, its local correlation with the global CO_2 level would not exist. Hence, the global CO_2 signal and the local temperature signal may be related but

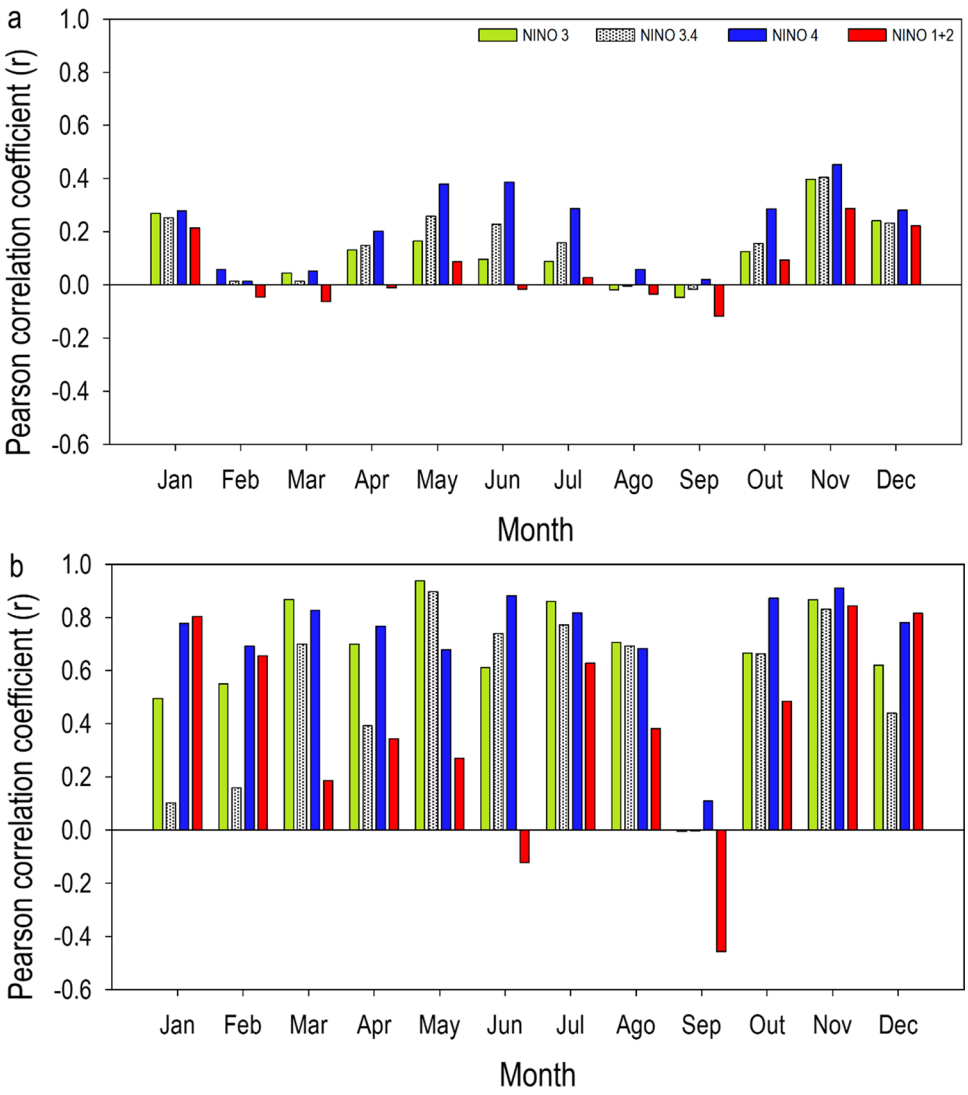

Fig. 11 Coefficient of correlation of monthly air temperature (T_{MAVE}) anomalies (baseline period: 1951–2000) between ESALQ's conventional weather station (CWS) and Niño SST indices regions (NOAA time series): **a** observed monthly; **b** 30-year moving average (1917–2016). Bar colors match with colors of Niño SST indices regions map (see Fig. 2)

they may also not be because they are two signals with different scales. We can therefore only note here the concordance between the two pieces of information but not make a statistical and even less mechanical link between the two. This means that the increase air temperature at local observations level may depend on many other factors beyond GHG levels.

As described previously, CWS has always been stationed within no-urban area and surely far away of urban–rural fringe (Trentin et al. 2015). Piracicaba region was largely deforested since at least 1940, and the weather station surrounding landscape since then has rural characteristics with a predominance of sugarcane and pastures, and small forest fragments (Sparovek and Costa, 2004). In a comprehensive analysis of the relationship between deforestation and air temperature in Brazil, Cohn et al. (2019) found that maximum air temperature can be expected to increase up to 0.95 °C in response decline in forest cover for a broad region; however, they also stated that previous studies could be wrongly mis-attributing warming to local change, where non-local changes also influence the pattern of temperature warming. More than 10 years ago, urban sprawl models indicated that the CWS site should be outside the main urban expansion vectors in Piracicaba City (Barretto et al. 2006). Based on MapBiomas data (https://mapbiomas.org/en, Souza et al. 2020), major changes in land use in the surrounding landscape (radius of 1784 m, area of 1000 ha) of the CWS were observed, as a trade-off from agricultural production area by the increasing of both forests and urban areas in the last 36 years (Fig. 14). The increases in the surrounding urban areas were mainly due to the expansion of university facilities and residential areas, while still preserving their rural characteristics, and still increasing the forest areas (Silva et al. 2006). These authors observed that annual increasing of the human discomfort bioclimatic index was linked

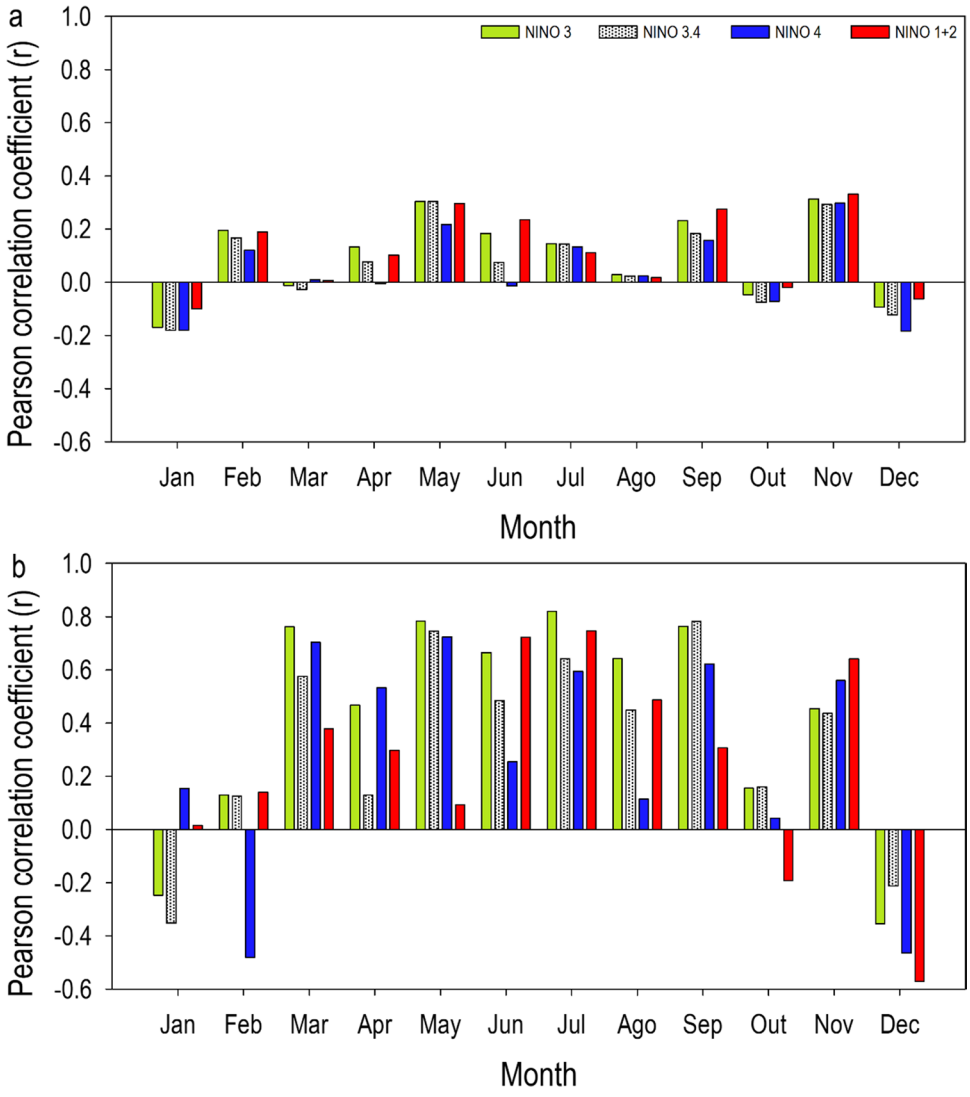

Fig. 12 Coefficient of correlation of rainfall (R_M) anomalies (baseline period: 1951–2000) between ESALQ's conventional weather station (CWS) and Niño SST indices regions (NOAA time series): **a** observed monthly; **b** 30-year moving average (1917–2016). Bar colors match with colors of Niño SST indices regions map (see Fig. 2)

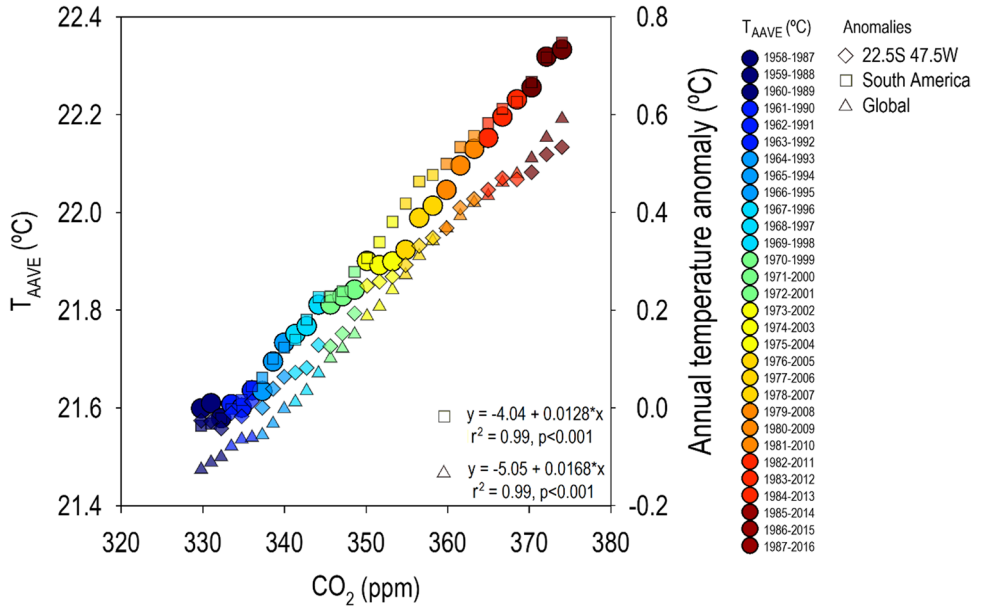

Fig. 13 Correlation between continental and global annual temperature anomalies (right y axis) from 1958–1987 to 1987–2016 (30-year moving average) and the long-term CO_2 air concentration observations from NOAA Lab in Mauna Loa, Hawaii, USA. Temperature data from other two different geographic data levels were plotted: Local = CWS air temperature (T_{AAVE}) (left y axis), Regional = annual temperature anomalies of CRUTEM4 grid-box (5° × 5°) with centroid of 22.5° South—47.5° West (Jones et al. 2012) (right y axis). Continental and global datasets are from Menne et al. (2018). CO_2 concentration is expressed as a mole fraction in dry air (μmol mol.$^{-1}$, abbreviated as ppm). We omitted from the graph the two curves of the relationship annual temperature anomalies and CO_2 concentration, keeping within graph only its equations and the statistical adjustment

with the land use changes on the Piracicaba, allowing them to state that accelerating land conversion is an important force that stimulates the local climate change.

Another key point for future studies of the centennial CWS dataset is consider that the land use and land cover is an important factor in determining the intensity of Urban Heat Islands (Monteiro et al. 2021) which would be forcing local climate changes. Blain et al. (2009) found contrasting results concerning the increasing of annual minimum temperatures across six distinct populated cities in São Paulo state, including Piracicaba, when analyzing long-term series until 2006. The effect of local radiative forcing seemed to

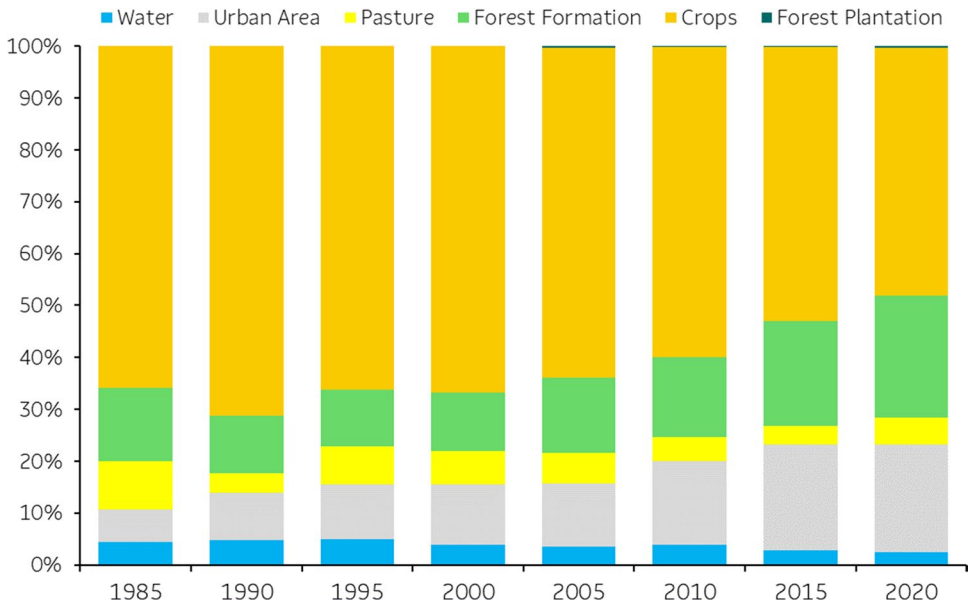

Fig. 14 Dynamics of land use changes observed in an area of 1000 ha (radius of 1784 m) around the conventional weather station (CWS) between 1985 and 2020. MapBiomas data (https://mapbiomas.org/en, Souza et al. 2020)

play a role in their results in places where urbanization is higher, but even in relatively low populated areas there were trends towards warming in other (Blain et al. 2009; Blain 2010). The series we analyzed included more 10 years when showed that such minimum temperatures kept increasing in Piracicaba, and the last 5 years (2017 to 2021) also show the same trend (data not shown). Disentangle the effects of local radiative forcing compared to regional and global changes deserves further investigation.

4 Conclusions

Our study provided a valid and strong scientific sound picture on climate change observed at Piracicaba, southeastern Brazil, over the last 100 years. The climate type in Piracicaba shifted from humid subtropical without dry season with hot summer (Cfa) to tropical with dry winter (Aw) when considering the last eight 30-year climatological normals, showing a clear tendency of tropicalization. It is important to emphasize that the results presented here represent only a very small sample of climate variability and change for one site. However, this is a contribution not only to reinforce the impacts of climate change at the local level, but also to show new possibilities of ways of visualizing meteorological data, their interrelationships, and insights. We hope that these deeper analyses will only improve over time, making the climate change subject easy to see and understand by the general population. In addition, our results also showed that relationships between local and global warming exist, but quantifying their anthropic or natural origin remains a challenge, and they are opportunities and should be better evaluated in future studies.

Ultimately, even under the inevitable tendency of automation of weather observations in Brazil and around the world, the ESALQ/USP conventional station remains in operation and is one of the few stations in the country with continuous long historical series of observations, which represents an important legacy for the history of meteorological observations in Brazil. We sincerely hope that the institution keeps this station active, serving as a reference for future generations to learn the importance of stations like that to monitor and understand climate variability and change in such region.

Acknowledgements We would like to express our gratitude to the two anonymous reviewers who contributed with great inputs to improve the earlier versions of this manuscript.

We are very grateful to all the professors, university staff, and students who have dedicated a lot of efforts to keep the Meteorological Observatory Professor Jesus Marden dos Santos from the "Luiz de Queiroz" College of Agriculture (ESALQ) of University of São Paulo (USP), data source of this study, in operation for more than 100 years. Indefatigable, Paulo Cesar Sentelhas was one of those distinguished professors who dedicated their entire academic life to keep the centennial weather station running.

Sadly, Professor Paulo Cesar Sentelhas passed away on 21 September 2021, due to complications from COVID-19. He first idealized this scientific contribution. Professor Sentelhas will be missed by many in Brazil and around the world due to his talent as teacher, scientist, and extensionist, in particular in the agrometeorology community. We, Clayton Alcarde Alvares and Henrique Boriolo Dias, dedicate this contribution to Paulo's memory.

Author contribution Conceptualization, methodology, validation, formal analysis, data curation, visualization, writing—original draft: C.A.A. Conceptualization, methodology, validation, formal analysis, data curation, writing—original draft: P.C.S. Conceptualization, data curation, validation, writing—review and editing: H.B.D.

Data availability All the climatic data used in this work is publicly available in the links provided throughout the article.

Code availability Code availability is not applicable to this article as no new code were create for this study.

Declarations

Ethics approval This article does not contain any studies with human or animal participants performed by any of the authors.

Consent to participate All authors have read and agreed to the published version of the article.

Consent for publication All authors have read and agreed to the published version of the article.

Conflict of interest The authors declare no competing interests.

References

Abreu RC, Tett SFB, Schurer A, Rocha HR (2019) Attribution of detected temperature trends in Southeast Brazil. Geophys Res Lett 46(14):8407–8414

Alvares CA, Stape JL, Sentelhas PC, Gonçalves JDM, Sparovek G (2013) Köppen's climate classification map for Brazil. Meteorol Z 22(6):711–728

Alvares CA, Sentelhas PC, Stape JL (2018) Modeling monthly meteorological and agronomic frost days, based on minimum air temperature. Center-Southern Brazil Theoretical and Applied Climatology 134(1):177–191

Alvares CA, Sentelhas PC, Chan CS (2021) Future climate projections in South America and their influence on forest plantations. IPEF, Piracicaba, Brazil

Barretto AGO, Sparovek G, Gianotti M (2006) Atlas rural de Piracicaba. Piracicaba: IPEF. 76p

Beck HE, Zimmermann NE, McVicar TR, Vergopolan N, Berg A, Wood EF (2018) Present and future Köppen-Geiger climate classification maps at 1-km resolution. Scientific Data 5(1):1–12

Becker A, Finger P, Meyer-Christoffer A, Rudolf B, Schamm K, Schneider U, Ziese M (2013) A description of the global land-surface precipitation data products of the Global Precipitation Climatology Centre with sample applications including centennial (trend) analysis from 1901–present. Earth System Science Data 5(1):71–99

Bezerra P, da Silva F, Cruz T, Mistry M, Vasquez-Arroyo E, Magalar L, ..., Schaeffer R (2021) Impacts of a warmer world on space cooling demand in Brazilian households. Energy and Buildings, 234, 110696

Bitencourt DP, Fuentes MV, Franke AE, Silveira RB, Alves MP (2020) The climatology of cold and heat waves in Brazil from 1961 to 2016. Int J Climatol 40(4):2464–2478

Blain GC, Picoli MCA, Lulu J (2009) Análises estatísticas das tendências de elevação nas séries anuais de temperatura mínima do ar no Estado de São Paulo. Bragantia 68(3):807–815. https://doi.org/10.1590/S0006-87052009000300030

Blain GC. Precipitação pluvial e temperatura do ar no Estado de São Paulo: periodicidades, probabilidades associadas, tendências e variações climáticas. Tese de Doutorado, Escola Superior de Agricultura "Luiz de Queiroz", Universidade de São Paulo, Piracicaba. https://doi.org/10.11606/T.11.2010.tde-24052010-155135

Braga B, Kelman J (2020) Facing the challenge of extreme climate: the case of Metropolitan Sao Paulo. Int J Water Resour Dev 36(2–3):278–291

Brasil (1970) Departamento de Meteorologia. Normais climatológicas: área do Nordeste do Brasil: período 1931–1960. Rio de Janeiro: Ministério da Agricultura. 91p.

Brasil (1992) Departamento de Meteorologia. Normais climatológicas 1961–1990. Rio de Janeiro: Ministério da Agricultura e Reforma Agrária. 91p

Cai W, McPhaden M, Grimm A, Rodrigues R, Taschetto A, Garreaud R, Dewitte B, Poveda G, Ham YG, Santoso A, Ng B, Anderson W, Wang G, Geng T, Jo H, Marengo J, Alves L, Osman M, Li S, Vera C (2020) Climate impacts of the El Niño-Southern Oscillation on South America. Nature Reviews Earth & Environment 1:215–231

Castellanos-Acuna D, Hamann A (2020) A cross-checked global monthly weather station database for precipitation covering the period 1901–2010. Geoscience Data Journal 7(1):27–37

Cavalcanti IFA, Marengo JA, Alves LM, Costa DF (2017) On the opposite relation between extreme precipitation over west Amazon and southeastern Brazil: observations and model simulations. Int J Climatol 37:3606–3618. https://doi.org/10.1002/joc.4942

Cavalcanti IFA, Kousky VE (2009) Cold fronts on Brazil. In: Cavalcanti IFA, Ferreira, NJ, Silva MGAJ, Dias MAFS (eds). Weather and Climate in Brazil. Oficina de Textos, São Paulo. pp 135–147

Chen D, Chen HW (2013) Using the Köppen classification to quantify climate variation and change: an example for 1901–2010. Environmental Development 6:69–79

Chou SC, Lyra A, Mourão C, Dereczynski C, Pilotto I, Gomes J, Bustamante J, Tavares P, Silva A, Rodrigues D, Campos D, Chagas D, Sueiro G, Siqueira G, Marengo J (2014) Assessment of climate change over South America under RCP 4.5 and 8.5 downscaling scenarios. Am J Clim Chang 3:512–527

Coelho CAS, de Oliveira CP, Ambrizzi T, Reboita MS, Carpenedo CB, Campos JLPS, Tomaziello ACN, Pampuch LA, Custódio MS, Dutra LMM, Rocha RP, Rehbein A (2016) The 2014 southeast Brazil austral summer drought: regional scale mechanisms and teleconnections. Clim Dyn 46:3737–3752. https://doi.org/10.1007/s00382-015-2800-1

Cohn AS, Bhattarai N, Campolo J, Crompton O, Dralle D, Duncan J, Thompson S (2019) Forest loss in Brazil increases maximum temperatures within 50 km. Environ Res Lett 14(8):084047

Cui D, Liang S, Wang D, Liu Z (2021) A 1-km global dataset of historical (1979–2017) and future (2020–2100) Köppen-Geiger climate classification and bioclimatic variables. Earth System Science Data Discussions, 1–34

Dias MAFS, Silva MGAJ (2009) Understanding Weather and Climate. In: Cavalcanti IFA, Ferreira, NJ, Silva MGAJ, Dias MAFS (eds). Weather and Climate in Brazil. Oficina de Textos, São Paulo. pp 15–21

Dias AP (1917) Meteorologia e Climatologia. São Paulo: Secção de Obras do "O Estado"

Díaz LB, Saurral RI, Vera CS (2021) Assessment of South America summer rainfall climatology and trends in a set of global climate models large ensembles. Int J Climatol 41:E59–E77

Diniz FDA, Ramos AM, Rebello ERG (2018) Brazilian climate normals for 1981–2010. Pesq Agrop Brasileira 53(2):131–143

Draenert, F.M. O clima do Brasil. Rio de Janeiro: Typographia Schmidt, p.63, 1896.

Dubreuil V, Fante KP, Planchon O, Sant'anna Neto JL (2019) Climate change evidence in Brazil from Köppen's climate annual types frequency. Int J Climatol 39(3):1446–1456

Fernandez JP, Franchito SH, Rao VB, Llopart M (2017) Changes in Koppen-Trewartha climate classification over South America from RegCM4 projections. Atmospheric Science Letters 18:427–434

Ferraz, M.S. Piracicaba e sua escola agrícola. Bruxeles: Imprimiere V. Verteneuil & L. Desmet. 1911.

Fick SE, Hijmans RJ (2017) WorldClim 2: new 1-km spatial resolution climate surfaces for global land areas. Int J Climatol 37(12):4302–4315

Geirinhas JL, Trigo RM, Libonati R, Coelho CA, Palmeira AC (2018) Climatic and synoptic characterization of heat waves in Brazil. Int J Climatol 38(4):1760–1776

Geirinhas JL, Russo A, Libonati R, Sousa PM, Miralles DG, Trigo RM (2021) Recent increasing frequency of compound summer drought and heatwaves in Southeast Brazil. Environ Res Lett 16(3):034036

Granato L (1913) Noções elementares de Meteorologia e Climatologia Agricola. Estab. Graphico Alongi & Gallo, São Paulo

Harris IPDJ, Jones PD, Osborn TJ, Lister DH (2014) Updated high-resolution grids of monthly climatic observations–the CRU TS3. 10 Dataset. Int J Climatol 34(3):623–642

Intergovernmental Panel on Climate Change – IPCC (2021) Climate Change 2021: The Physical Science Basis. Contribution of Working Group I to the Sixth Assessment Report of the Intergovernmental Panel on Climate Change [Masson-Delmotte, V., P. Zhai, A. Pirani, S.L. Connors, C. Péan, S. Berger, N. Caud, Y. Chen, L. Goldfarb, M.I. Gomis, M. Huang, K. Leitzell, E. Lonnoy, J.B.R. Matthews, T.K. Maycock, T. Waterfield, O. Yelekçi, R. Yu, and B. Zhou (eds.)]. Cambridge University Press. In Press.

Jones PD, Lister DH, Osborn TJ, Harpham C, Salmon M, Morice CP (2012) Hemispheric and large-scale land surface air temperature variations: an extensive revision and an update to 2010. J Geophys Res 117:D05127. https://doi.org/10.1029/2011JD017139

Köppen W (1936) Das geographische System der Klimate – Köppen, W.; GEiger, R. (Eds): Handbuch der Klimatologie – Gebrüder Borntträger, Berlin, 1, 1–44, part C

Marengo JA, Ambrizzi T, Lincoln MA, Barreto NJ, Reboita MS, Ramos AM (2020) Changing trends in rainfall extremes in the metropolitan area of São Paulo: causes and impacts. Front Clim 2(3)

Menne MJ, Williams CN, Gleason BE, Rennie JJ, Lawrimore JH (2018) The Global Historical Climatology Network Monthly Temperature Dataset, Version 4. J Clim 31(24):9835–9854

Monteiro FF, Gonçalves WA, Andrade LDMB, Villavicencio LMM, dos Santos Silva CM (2021) Assessment of Urban Heat Islands in Brazil based on MODIS remote sensing data. Urban Climate 35:100726

Morize H (1927) Contribuição ao estudo do clima do Brasil. Ministério da Agricultura, Indústria e Commercio. Observatório Nacional do Ri ode Janeiro. Typographia do Serviço de Informações do Ministério de Agricultura. Rio de Janeiro, 116 p

Nobre CA, Marengo JA, Seluchi ME, Cuartas LA, Alves LM (2016) Some characteristics and impacts of the drought and water crisis in Southeastern Brazil during 2014 and 2015. J Water Resour Prot 8(2):252–262

Oliveira Souza TC, Delgado RC, Magistrali IC, dos Santos GL, de Carvalho DC, Teodoro PE, da Silva Júnior CA, Caúla RH (2018) Spectral trend of vegetation with rainfall in events of El Niño-Southern Oscillation for Atlantic Forest biome. Brazil Environ Monit Assess 190:688. https://doi.org/10.1007/s10661-018-7060-1

Peel MC, Finlayson BL, McMahon TA (2007) Updated world map of the Köppen-Geiger climate classification. Hydrol Earth Syst Sci 11(5):1633–1644

Pereira AR. Angelocci LR, Sentelhas PC (2002) Agrometeorologia: fundamentos e aplicações práticas. Livraria e Editora Agropecuária, Guaíba, Brazil

Ramos AM, Santos LAR, Fortes LTG (eds) (2009) Normais climatológicas do Brasil 1961–1990. Instituto Nacional de Meteorologia-INMET, Ministério da Agricultura, Pecuária e Abastecimento-MAPA. Brasília, DF, p 465

Regoto P, Dereczynski C, Chou SC, Bazzanela AC (2021) Observed changes in air temperature and precipitation extremes over Brazil. Int J Climatol; 1– 18. https://doi.org/10.1002/joc.7119

Saurral RI, Camilloni IA, Barros VR (2017) Low-frequency variability and trends in centennial precipitation stations in southern South America. Int J Climatol 37(4):1774–1793

Sentelhas PC, Moraes SO, Piedade SDS, Pereira AR, Angelocci LR, Marin FR (1997) Análise comparativa de dados meteorológicos obtidos por estações convencional e automática. Revista Brasileira De Agrometeorologia, Santa Maria 5(2):215–221

Seth A, Fernandes K, Camargo SJ (2015) Two summers of São Paulo drought: Origins in the western tropical Pacific. Geophys Res Lett 42(24):10–816

Setzer J (1946) Contribuição para o estudo do clima do Estado de São Paulo. Escolas Profissionais Salesianas, São Paulo, Brasil, 239 p

Silva AM, Moraes JM, Ferraz ESB, Alvares CA (2006) Bioclimatic characterization and trend analysis of the discomfort index for Piracicaba-SP. Geografia 31:151–167

Souza CM, Shimbo JZ, Rosa MR, Parente LL, Alencar AA, Rudorff BFT et al (2020) Reconstructing three decades of land use and land cover changes in Brazilian biomes with landsat archive and earth engine. Remote Sens 12:2735. https://doi.org/10.3390/rs12172735

Sparovek G, Costa FPS (2006) Evolução da cobertura vegetal da cidade de Piracicaba-SP (1940–2000). Geografia 31:331–346

Trentin G, Mattos ECA, Ferreira MC (2015) Caracterização e delimitação da região de entorno imediato (rei) de áreas urbanas: um estudo para a área urbana de Piracicaba-SP. Rev Bras Cartogr 67:631–635

Venegas-González A, Roig FA, Lisi CS, Albiero-Junior A, Alvares CA, Tomazello-Filho M (2018) Drought and climate change incidence on hotspot Cedrela forests from the Mata Atlântica biome in southeastern Brazil. Global Ecology and Conservation 15:e00408

Wang M, Overland JE (2004) Detecting Arctic climate change using Köppen climate classification. Clim Change 67:43–62. https://doi.org/10.1007/s10584-004-4786-2

WMO – World Meteorological Organization - What is the difference between Climate Variability and Climate Change?. Accessed in 04 Nov 2020. www.https://wmo.int.

Xavier AC, King CW, Scanlon BR (2016) Daily gridded meteorological variables in Brazil (1980–2013). Int J Climatol 36(6):2644–2659

Xue X, Ren G, Sun X, Zhang P, Ren Y, Zhang S ..., Yu X (2021) Change in mean and extreme temperature at Yingkou station in Northeast China from 1904 to 2017. Climatic Change 164(3):1-20